bias voltage, but leads to a correlation between the RF component of AM and FM noise. This is because both quadrature components of RF noise contribute to FM noise when the device admittance is RF and bias voltage dependent. Further, the video component of FM noise is altered by the RF-voltage dependence.

The results indicate that device fabrication for lowest noise performance should not only be directed toward improved processing techniques which reduce crystal imperfections and surface traps, both of which lead to high $1/f$ noise, but also toward tailoring the device admittance curves so that at the desired operating point for a particular application the RF-voltage variation cf the admittance is large and the bias-voltage variation is small.

Acknowledgment

The author wishes to thank Dr. W. R. Curtice for his contributions to this work.

References

[1] W. A. Edson, "Noise in oscillators," *Proc. IRE*, vol. 48, pp. 1454–1466, August 1960.
[2] J. A. Mullen, "Background noise in nonlinear oscillators," *Proc. IRE*, vol. 48, pp. 1467–1473, August 1960.
[3] B. van der Pol, "The nonlinear theory of electric oscillations," *Proc. IRE*, vol. 22, pp. 1051–1086, September 1934.
[4] M. Lax, "Classical noise. V. Noise in self-sustained oscillators," *Phys. Rev.*, vol. 160, pp. 290–307, August 10, 1967.
[5] K. Kurokawa, "Noise in synchronized oscillators," *IEEE Trans. Microwave Theory Tech.*, vol. MTT-16, pp. 234–240, April 1968.
[6] W. Schockley, J. A. Copeland, and R. P. James, "The impedance field method of noise calculation in active semiconductor devices," in *Quantum Theory of Atoms, Molecules, and the Solid State*. New York: Academic, 1966.
[7] H. J. Thaler, G. Ulrich, and G. Wiedmann, "Noise in IMPATT diode amplifiers and oscillators," *IEEE Trans. Microwave Theory and Tech.*, vol. MTT-19, pp. 692–706, August 1971.
[8] M. T. Vlaardingerbrock and J. J. Goedbloed, "On the theory of noise in IMPATT diode oscillators," *Philips Research Report*, vol. 25, pp. 452–471, 1970.
[9] K. Mouthaan and H. J. M. Rijpert, "Non-linearity and noise in the A.T.T. oscillator," *Philips Research Report*, vol. 26, pp. 394–413, 1971.
[10] J. J. Goedbloed, "On the up-converted noise of IMPATT diode oscillators," *Proc. of MOGA Conf.*, Amsterdam, pp. 12.36–12.40, 1970.
[11] ——, "FM noise of low level operating IMPATT diode oscillators," *Electronics Letters*, vol. 7, no. 16, pp. 445–446, August 12, 1961.
[12] G. Convert, "A non-linear theory of noise in Read diodes," *Proc. IEEE*, vol. 59, pp. 1266–1267, August 1971.
[13] M. T. Vlaardingerbrock, "Theory of oscillator noise," *Electronics Letters*, vol. 7, no. 21, pp. 648–650, October 21, 1971.
[14] A. A. Sweet, "A general analysis of noise in Gunn oscillators," *Proc. IEEE* (Letters), vol. 60, pp. 999–1000, August 1972.
[15] H. A. Haus, H. Statz, and R. A. Pucel, "Noise in Gunn oscillators," *IEEE Trans. Electron Devices*, vol. ED-20, pp. 368–370, April 1973.
[16] W. B. Davenport, Jr., *Probability and Random Processes: An Introduction for Applied Scientists and Engineers*. New York: McGraw-Hill, 1970.
[17] A. Papoulis, *Probability, Random Variables and Stochastic Processes*. New York: McGraw-Hill, pp. 430–452, 1965.

On Some Integral Relationships for Commensurate Transmission-Line Networks

EDWARD G. CRISTAL, SENIOR MEMBER, IEEE

***Abstract*—Several integral relationships are presented for commensurate transmission-line networks. The integrals focus on the fact that $Z(1)$ for such networks, where $Z(S)$ is the input immittance of the network, is associated with a real or redundant unit element prefacing the network. Three bandwidth restrictions are derived. Some applications of the integral relationships are presented.**

Manuscript received July 17, 1975; revised January 12, 1976.

The author is with the Hewlett-Packard Company, Palo Alto, CA 94304.

For commensurate transmission-line networks it is convenient to use Richards [1] variable S, where

- S tanh $\{\tau s/2\} = \sum + i\Omega$;
- τ $2l/v$, the round-trip delay for the shortest commensurate length line;
- l length of the shortest commensurate length line;
- v velocity of propagation;
- s $\sigma + i\omega$, the complex frequency variable of lumped-element networks.

Richards proved that driving-point immittances (impedances or admittances) $Z(S)$ are rational functions of S and are positive real. In this short paper we consider several integral relationships for general immittance functions $Z(S)$ expressible in the form

$$Z(S) = F(S) + M(S)$$

$$F(S) = \text{Foster preamble}$$

$$= A_1{}^{\infty} S + \frac{A_{-1}{}^0}{S} + \sum_{k=1}^{L} \frac{2A_{-1}{}^k S}{S^2 + \Omega_k{}^2}$$

$$M(S) = \frac{a_0 + a_1 S + a_2 S^2 + \cdots + a_n S^n}{b_0 + b_1 S + b_2 S^2 + \cdots + b_m S^m}, \qquad n = m \text{ or } m-1.$$

Also, at infinity, $M(S)$ can be expanded into

$$\lim_{S\to\infty} M(S) = m_\infty + \frac{m_{-1}}{S} + \frac{m_{-2}}{S^2} + \cdots.$$

The first integral, and one of primary interest, is

$$\oint_C \frac{Z(S)}{S^2 - 1}\, dS \tag{1}$$

where C is the Bromwich [2] contour consisting of the $\sum = 0$ axis, and the infinite semicircle enclosing the RHP. By Cauchy's theorem, (1) is

$$\pi i Z(1) = \int_{i\infty}^{-i\infty} \frac{Z(i\Omega) i\, d\Omega}{-\Omega^2 - 1} + \oint_{-\pi/2}^{\pi/2} \frac{Z(S)\, dS}{S^2 - 1}.$$

Details of evaluating the RHS of the previous equation are given in the Appendix. The final result is

$$Z(1) = \frac{2}{\pi}\int_0^\infty \frac{R(\Omega)\, d\Omega}{\Omega^2 + 1} + A_1{}^\infty + A_{-1}{}^0 + 2\sum_{k=1}^{L} \frac{A_{-1}{}^k}{1 + \Omega_k{}^2} \tag{2}$$

where $R(\Omega) + iX(\Omega) = Z(i\Omega)$. On the "real-frequency axis"

$$S = i\Omega = i \tan\theta$$

where $\theta = \omega l/v$ is the electrical length. Substitution into (2) results in

$$Z(1) = \frac{2}{\pi}\int_0^{\pi/2} R(\theta)\, d\theta + A_1{}^\infty + A_{-1}{}^0 + 2\sum_{k=1}^{L} \frac{A_{-1}{}^k}{1 + \Omega_k{}^2}. \tag{3}$$

The integral on the RHS of (3) is the average of $R(\theta)$ over $\pi/2$ rad. Hence, transposing, (3) states

$$R_{\text{avg}} = Z(1) - 2\sum_{k=1}^{L} \frac{A_{-1}{}^k}{1 + \Omega_k{}^2} - A_{-1}{}^0 - A_1{}^\infty. \tag{4}$$

Thus, the average value of the real part of $Z(S)$ over $\pi/2$ rad equals $Z(1)$ less the weighted values of the residues of its Foster preamble. Equations (2)–(4) are particularly useful forms since

$Z(1)$ can be interpreted as the characteristic immittance of a unit element [3] prefacing the Z network.

Weak-Limit Bandwidth Laws

Equations (3) and (4) may be used to derive a "weak-limit" bandwidth law applicable to all networks having a positive-real input immittance, and a less general weak-limit bandwidth law applicable to a restricted class of networks.

Assume a voltage source E_g having internal resistance R_1 delivering energy to an arbitrary network N having a positive-real input immittance. The available power from the source is $E_g^2/4R_1$. The power into N is $E_g^2 R_{in}/|R_1 + R_{in} + jX_{in}|^2$. The ratio of input to available power is

$$P_{in}/P_{avail} = \frac{4R_1 R_{in}}{|R_1 + R_{in} + jX_{in}|^2} = \frac{4r_{in}}{|1 + r_{in} + jx_{in}|^2} \tag{5}$$

with $r_{in} = R_{in}/R_1$ and $x_{in} = X_{in}/R_1$. Integrating (5) from 0 to $\pi/2$ and multiplying by $2/\pi$ gives

$$\frac{2}{\pi}\int_0^{\pi/2} P_{in}/P_{avail}\, d\theta = \frac{2}{\pi}\int_0^{\pi/2} \frac{4r_{in}\, d\theta}{|1 + r_{in} + jx_{in}|^2} \leq \frac{2}{\pi}\int_0^{\pi/2} \frac{4r_{in}\, d\theta}{(1 + r_{in})^2}. \tag{6}$$

In order to utilize (4), the RHS of (6) is replaced by the weaker inequality

$$\frac{2}{\pi}\int_0^{\pi/2} \frac{4r_{in}\, d\theta}{(1 + r_{in})^2} \leq \frac{2}{\pi}\int_0^{\pi/2} Mr_{in}\, d\theta + U(M) \tag{7}$$

where

M slope of the linear function Mr_{in};
$U(M)$ maximum of $\{4r_{in}/(1 + r_{in})^2 - Mr_{in}\}$ on $r_{in} \geq 0$.

The function $U(M)$ can be interpreted as the maximum uncertainty in replacing

$$\frac{2}{\pi}\int_0^{\pi/2} \frac{4r_{in}\, d\theta}{(1 + r_{in})^2}$$

by

$$\frac{2}{\pi}\int_0^{\pi/2} Mr_{in}\, d\theta.$$

Combining (4), (6), and (7) gives

$$\frac{2}{\pi}\int_0^{\pi/2} P_{in}/P_{avail}\, d\theta = \{P_{in}/P_{avail}\}_{avg} \leq \frac{M}{R_1}\left\{Z(1) - A_1^{\infty} - A_{-1}^{0} - 2\sum_{k=1}^{L} \frac{A_{-1}^{k}}{(1 + \Omega_k^2)}\right\} \tag{8}$$

with a maximum uncertainty of $U(M)$.[1]

By the same procedures but on an admittance basis we obtain

$$\frac{2}{\pi}\int_0^{\pi/2} P_{in}/P_{avail}\, d\theta = \{P_{in}/P_{avail}\}_{avg} \leq \frac{\bar{M}}{G_1}\left\{Y(1) - B_1^{\infty} - B_{-1}^{0} - 2\sum_{k'=1}^{L'} \frac{B_{-1}^{k'}}{(1 + \Omega_{k'}^2)}\right\} \tag{9}$$

[1] It is shown later how to choose an optimum M.

with a maximum uncertainty of $U(\bar{M})$. Because the imaginary part of the input immittance of N cannot in general be cancelled, and because (7) is typically a weak inequality, (8) and (9) have been designated as weak-limit bandwidth laws. *Define the term "weak-limit" as the smaller of the RHS of (8) and (9).* Then the weak-limit bandwidth law can be stated succinctly as follows.

The averaged normalized power into an arbitrary network having a positive-real input immittance is less than or equal the weak limit. Mathematically,

$$\frac{2}{\pi}\int_0^{\pi/2} P_{in}/P_{avail}\, d\theta \leq \text{the weak limit.} \tag{10}$$

If the network N represents a lossless 2-port terminated in a resistive load, the power into N must be absorbed by the load. In that case, the integrand on the LHS of (10) is the absolute value squared of the 2–1 scattering coefficient. Thus, for lossless networks N, the weak-limit bandwidth law is

$$\frac{2}{\pi}\int_0^{\pi/2} |S_{21}|^2\, d\theta \leq \text{the weak limit.} \tag{11}$$

The lowest bound in the weak limit is obtained as follows. Note in (8) and (9) that the weak limit is of the form

$$\text{weak limit} = Mx + U(M).$$

Consequently, for a given x the lowest bound occurs for an M satisfying

$$\frac{dU}{dM} + x = 0$$

or

$$x = -\frac{dU}{dM}.$$

For convenience in solving the previous equation, $-dU/dM$ is plotted in Fig. 1. The uncertainty function $U(M)$ is given in Fig. 2. Note that both functions are monotonic decreasing from 1 to 0 as M ranges from 0 to 4.

Therefore, knowing x, a value of M_0 is obtained from Fig. 1, and the value $U(M_0)$ from Fig. 2. Then the lowest bound on the weak-limit is

$$M_0 x + U(M_0).$$

A second weak-limit bandwidth law can be derived for networks where the input immittance has nonzero real part and no poles or zeros on the $j\Omega$ axis. In these cases

$$\frac{2}{\pi}\int_0^{\pi/2} P_{avail}/P_{in}\, d\theta = \frac{2}{\pi}\int_0^{\pi/2} \frac{|1 + r_{in} + jx_{in}|^2}{4r_{in}} \geq \frac{2}{\pi}\int_0^{\pi/2} \frac{(1 + r_{in})^2}{4r_{in}}\, d\theta. \tag{12}$$

Now, $1/r_{in} = (g_{in}^2 + b_{in}^2)/g_{in} \geq g_{in}$. Thus

$$\frac{2}{\pi}\int_0^{\pi/2} \frac{(1 + r_{in})^2\, d\theta}{4r_{in}} \geq \frac{2}{\pi}\int_0^{\pi/2} \frac{g_{in}(1 + r_{in})^2\, d\theta}{4}.$$

Substituting into (12) gives the weaker inequality

$$\frac{2}{\pi}\int_0^{\pi/2} P_{avail}/P_{in}\, d\theta \geq \frac{1}{4}\left\{\frac{2}{\pi}\int_0^{\pi/2} (g_{in} + 2 + r_{in})\, d\theta\right\}. \tag{13}$$

Combining (13) and (4)

$$\frac{2}{\pi}\int_0^{\pi/2} P_{avail}/P_{in}\, d\theta \geq \tfrac{1}{4}\{y(1) + 2 + z(1)\}.$$

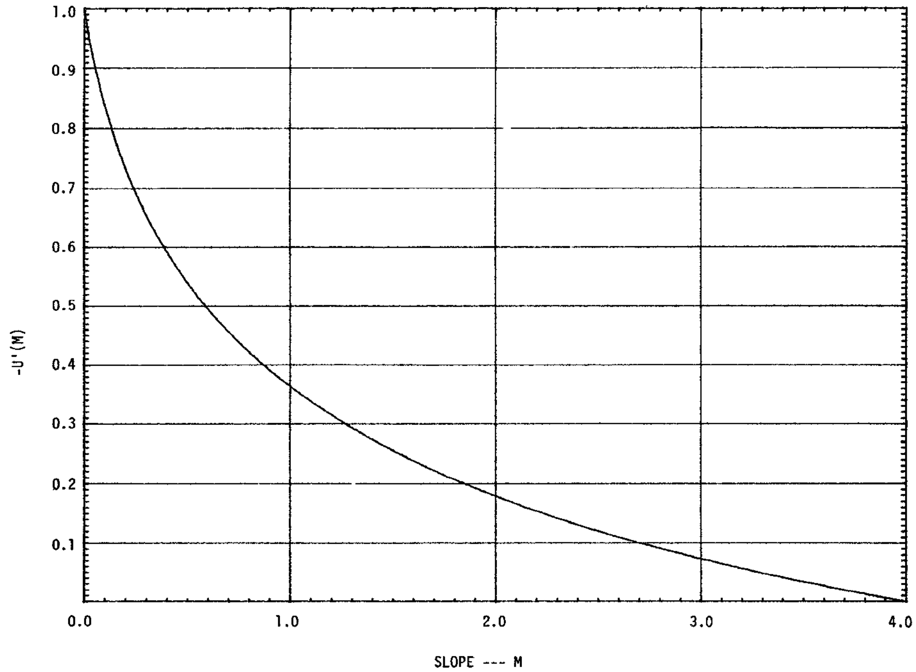

Fig. 1. Minus the derivative of the uncertainty function versus M.

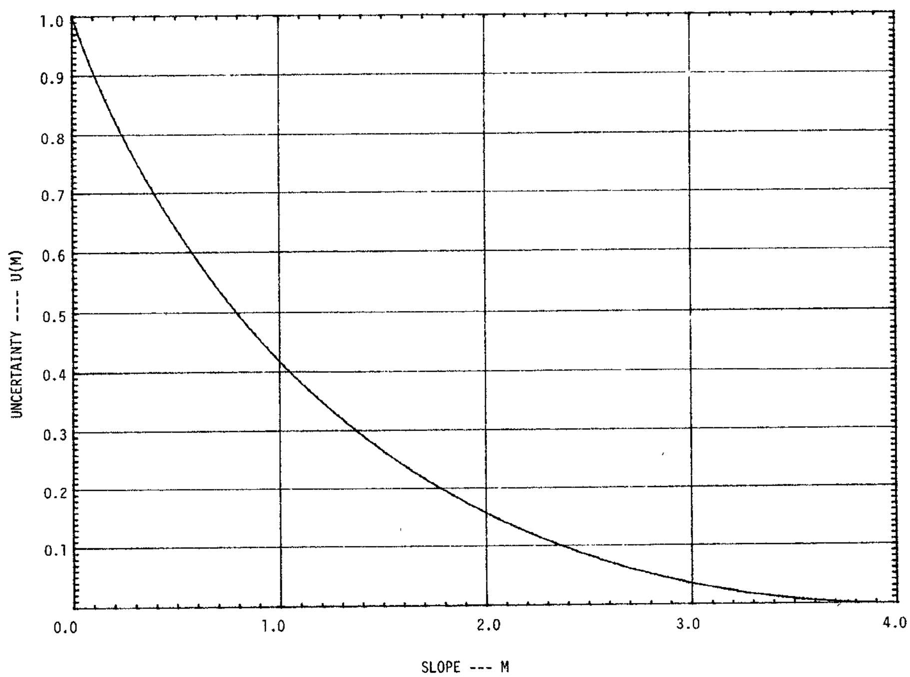

Fig. 2. Uncertainty function $U(M)$ versus M.

But $y(1) = 1/z(1)$. Thus, after simplification, the final inequality is

$$\frac{2}{\pi}\int_0^{\pi/2} P_{\text{avail}}/P_{\text{in}}\, d\theta \geq \frac{(1 + z(1))^2}{4z(1)}. \tag{14}$$

Equation (14) has the advantage over (8) and (9) in that there is no additional uncertainty function. However, it is valid only for a restricted class of network immittances.

In view of the previous results, it is perhaps instructive to look at a specific example. Let $R_1 = 1\ \Omega$, and network N be a 2-section quarter-wave transformer terminated in a 10-Ω resistance. Young's tables [4] give $Z(1) = 1.794$. The LHS of (10) was evaluated by dividing the interval 0 to $\pi/2$ into 18 equal segments and using Simpson's quadrature on the analytical (Chebyshev) response. The result was LHS = 0.676. The least weak limit is obtained by using Fig. 1 to solve

$$-\frac{dU}{dM} = 1/1.794 = 0.557.$$

The answer is $M_0 = 0.47$. From Fig. 2, $U(M_0 = 0.47) = 0.655$. Thus

weak limit = 0.47(0.557) + an uncertainty of 0.655

or

$$\text{least weak limit} = 0.262 + 0.655 = 0.917.$$

Thus the LHS is somewhat less than the weak limit, as anticipated.

Inequality (14) is also applicable to this example. By similar numerical procedures the LHS of (14) was found to be 1.753. The RHS is 1.088. Thus (14) is also easily satisfied.

Return-Loss Bandwidth Restriction

Using the previous results, the average return loss may be computed. We consider the integral

$$\oint \frac{\ln \Gamma(S)}{S^2 - 1} \, dS \tag{15}$$

where $\Gamma(S)$ is the reflection coefficient of a given network N. The reflection coefficient may be expressed

$$\Gamma(S) = A \frac{\prod_i (S - z_i)}{\prod_k (S - p_k)} \tag{16}$$

where z_i, p_k are in general complex, Re $(p_k) < 0$, but the Re (z_i) unrestricted. It can be shown that the same final result is obtained for negative A as positive A. We treat the latter case here. Two separate cases are considered.

Case I: Re $(z_i) < 0$ for all i. Then, by (4),

$$\frac{2}{\pi} \int_0^{\pi/2} \ln |\Gamma(\theta)| \, d\theta = \ln |\Gamma(1)|. \tag{17}$$

Case II: Re $(z_i) > 0$ for $I \leq i \leq I'$. In this case, following Bode's procedure [5], we form

$$\hat{\Gamma}(S) = \Gamma(S) \prod_{i=I}^{I'} \frac{(S + z_i)}{(S - z_i)}. \tag{18}$$

Note that

$$|\hat{\Gamma}(S)| = |\Gamma(S)| \quad \text{for} \quad S = i\Omega.$$

Therefore, by (4),

$$\frac{2}{\pi} \int_0^{\pi/2} \ln |\Gamma(\theta)| \, d\theta = \ln |\Gamma(1)| + \ln \left| \prod_{i=I}^{I'} \frac{1 + z_i}{1 - z_i} \right|. \tag{19}$$

The first term on the RHS of (19) is always less than zero, while the second term on the RHS of (19) is always greater than zero. Thus Cases I and II can be conveniently expressed in the single inequality

$$\frac{2}{\pi} \int_0^{\pi/2} \ln \left| \frac{1}{\Gamma(\theta)} \right| d\theta \leq \ln \left| \frac{1}{\Gamma(1)} \right|. \tag{20}$$

Equation (20) states: *the average return loss in nepers over $\pi/2$ rad is less than or equal the return loss at $S = 1$.*

It is interesting to note that if the first element of the network N is a unit element of characteristic impedance Z, the average return loss cannot exceed

$$\ln \left| \frac{Z + 1}{Z - 1} \right| \tag{21}$$

regardless of the remainder of N.

An important consequence can be drawn from these results regarding the bandwidth of cascaded, stepped-impedance transformers and directional couplers. For impedance transformers one desires to minimize Γ over the matching bandwidth. However, the average return loss cannot exceed (21). Thus, the gain-bandwidth performance of the transformer is limited (at least) by the impedance levels of the *first* and *last* quarter-wavelength lines.

For a cascaded directional coupler, Γ for the even-mode input impedance is in one-to-one correspondence with the coupling coefficient of the coupler. In this case, one wishes Γ to be constant over as wide a bandwidth as possible. But, again, the average coupling (ln $|1/\Gamma|$) cannot exceed (21). Thus the bandwidth of the coupler is limited (at least) by the even-mode impedance of the *first* and *last* coupling sections. The aforementioned limits may be weak limits depending on the zeros of the reflection coefficient, but in all cases they cannot be exceeded.

Measurement Applications

In addition to providing bandwidth information on Z, (2)–(4) can be utilized in certain measurement methods. For example, (3) and (4) suggest a simple CW procedure for measuring the characteristic impedance of an unknown transmission line. Consider a transmission line of unknown characteristic impedance R_x terminated in an arbitrary real load R_L. At a suitable reference plane

$$Z(S) = R_x \frac{R_L + R_x S}{R_x + R_L S} = M(S)$$

in this case, $A_{-1}{}^0 = A_1{}^\infty = A_{-1}{}^k = 0$. Therefore,

$$Z(1) = R_x = \frac{2}{\pi} \int_0^{\pi/2} R(\theta) \, d\theta = R_{\text{avg}}.$$

Thus a measurement of $R(\theta)$ averaged over $\pi/2$ rad equals the characteristic impedance of the line. Note that knowledge of the value of R_L is not required. An advantage of this CW approach is that averaging the measurements tends to reduce random measurement errors.

For a second example, consider a network consisting of a line (characteristic impedance R) terminated by a shunt stub (characteristic admittance C) in parallel with a real load R_L. Evaluation of (4) for the average of R_{in} and G_{in} yields

$$\{R_{\text{in}}\}_{\text{avg}} = R/(1 + RC)$$

$$\{R_{\text{in}}\}_{\text{avg}}^{-1} = G + C, \qquad (G = 1/R) \tag{22}$$

$$\{G_{\text{in}}\}_{\text{avg}} = G. \tag{23}$$

A possible application of the latter results is to the experimental determination of self- and mutual-capacitance (and hence coupling) of some coupled-line geometries. Consider the network shown in Fig. 3. The relationships between the equivalent-circuit parameters (which correspond to the current example) and the coupled-line capacitance parameters are

$$vC_{11} = G + C \tag{24}$$

$$vC_{12} = \sqrt{C(G + C)}. \tag{25}$$

Thus CW measurements of $\{R_{\text{in}}\}_{\text{avg}}$ and $\{G_{\text{in}}\}_{\text{avg}}$ together with (22)–(25) yield the coupled-line parameters. Numerous other examples are possible.

Additional Integral Relationships

Other potentially useful integral relationships may be established by selecting other integrands. Three are given as follows:

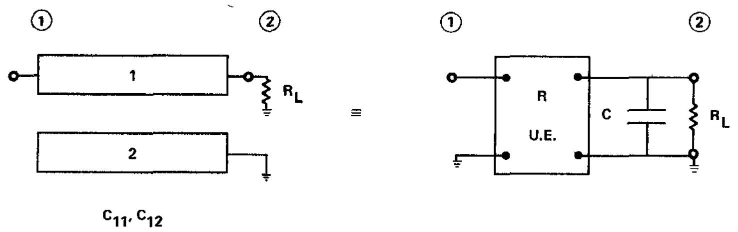

Fig. 3. Symmetrical coupled-line geometry and equivalent circuit.

for the integrand of

$$\frac{S[Z(S) - A_1^{\infty}S]}{S^2 - 1}$$

the result is

$$Z(1) - A_1^{\infty} = -\frac{2}{\pi}\int_0^{\infty} \frac{\Omega X(\Omega) - \Omega^2 A_1^{\infty}}{1 + \Omega^2}\, d\Omega + m_{\infty}. \quad (26)$$

If $F(S) \equiv 0$, for an integrand of $M^2(S)/[S^2 - 1]$, the result is

$$M^2(1) = \frac{2}{\pi}\int_0^{\pi/2} [R^2(\theta) - X^2(\theta)]\, d\theta. \quad (27)$$

For an integrand of $[M(S) - m_{\infty}]^2/[S^2 - 1]$, the result is

$$[M(1) - m_{\infty}]^2 = \frac{2}{\pi}\int_0^{\pi/2} [R(\theta) - R(\pi/2)]^2 - X^2(\theta)\, d\theta. \quad (28)$$

Equation (26) involves solely the imaginary part of Z_{in}, but the integrand cannot be conveniently transformed into a function of θ. Equations (27) and (28) interrelate the real and imaginary parts of Z_{in}. Equation (27) is interesting in that it reveals that the difference in the average of R_{in}^2 and X_{in}^2 is exactly equal to $[Z(1)]^2$ for cases where Z has no Foster preamble.

Conclusions

Use of the weighting function $(S^2 - 1)^{-1}$ in contour integrals of positive-real network immittance functions resulted in several new network interrelationships and 3 bandwidth constraints. The integral relationships can be used in the CW determination of network parameters in certain cases. Some specific results were as follows.

1) For a network preceded by a unit element, the average real part of the input immittance is less than, or equal to, the characteristic immittance of the unit element.

2) In general, the average of the real part of the input immittance $Z(S)$ is equal to $Z(1)$ less the weighted residues of its Foster preamble.

3) In general,

$$\frac{2}{\pi}\int_0^{\pi/2} P_{\text{in}}/P_{\text{avail}}\, d\theta \le \text{the weak limit (as defined in the text).}$$

4) For networks whose input immittance has nonzero real part and no poles or zeros on the $j\Omega$ axis,

$$\frac{2}{\pi}\int_0^{\pi/2} P_{\text{avail}}/P_{\text{in}}\, d\theta \ge \frac{[1 + z(1)]^2}{4z(1)}.$$

5) In general,

$$\frac{2}{\pi}\int_0^{\pi/2} \ln\left|\frac{1}{\Gamma(\theta)}\right| d\theta \le \ln\left|\frac{1}{\Gamma(1)}\right|.$$

Appendix

Let $Z(S) = F(S) + M(S)$ be a positive-real immittance defined in the text. By Cauchy's theorem

$$\oint_C \frac{Z(S)}{S^2 - 1}\, dS = i\pi Z(1) \quad \text{(A-1)}$$

where C is the Bromwich contour consisting of the $\sum = 0$ axis and the infinite semicircle enclosing the RHP. The LHS of (A-1) expands to

$$\int_{i\infty}^{-i\infty} \frac{R(i\Omega) + iX(i\Omega)}{-\Omega^2 - 1}\, i\, d\Omega + \int_{-\pi/2}^{\pi/2} \frac{Z(S)}{S^2 - 1}\, dS. \quad \text{(A-2)}$$

On the $i\Omega$ axis R is even and X is odd so that the first term in (A-2) simplifies to

$$2i\int_0^{\infty} \frac{R(\Omega)}{\Omega^2 + 1}\, d\Omega. \quad \text{(A-3)}$$

At complex conjugate poles, $\pm i\Omega_k$, $Z(S)$ may be written

$$Z(S) = \frac{2A_{-1}{}^k S}{S^2 + \Omega_k{}^2} + \bar{Z}(S). \quad \text{(A-4)}$$

In the vicinity of the imaginary axis conjugate poles, the paths of integration are infinitesimal semicircles of radius r, centered at the poles, and extending into the RHP. The contribution from the semicircular path at $S = i\Omega_k$ is

$$\lim_{r \to 0} \int_{\pi/2}^{-\pi/2} \left\{\frac{2A_{-1}{}^k S}{S^2 + \Omega_k{}^2} + \bar{Z}(S)\right\} \frac{dS}{S^2 - 1} \quad \text{(A-5)}$$

with $S = r \exp(i\theta) - i\Omega_k$, and $dS = ir \exp(i\theta)\, d\theta$. In the limit (A-5) equals $i\pi A_{-1}{}^k/(\Omega_k{}^2 + 1)$. At the conjugate pole there is an equal contribution so that the total for L conjugate poles on the imaginary axis is

$$i2\pi \sum_{k=1}^{L} \frac{A_{-1}{}^k}{1 + \Omega_k{}^2}. \quad \text{(A-6)}$$

For a pole at the origin the corresponding integral is

$$\lim_{r \to 0} \int_{\pi/2}^{-\pi/2} \left\{\frac{A_{-1}{}^0}{S} + \hat{Z}(S)\right\} \frac{dS}{S^2 - 1}$$

and its contribution is

$$i\pi A_{-1}{}^0. \quad \text{(A-7)}$$

The second term of (A-2) is evaluated by selecting a finite semicircular contour of radius r, centered at the origin, and taking the limit as $r \to \infty$. For large S, $Z(S)$ can be expanded

$$Z(S) = A_1^{\infty}S + m_{\infty} + \tilde{Z}(S).$$

Substitution into the second term of (A-2) gives

$$\lim_{r\to\infty} \int_{-\pi/2}^{\pi/2} \{A_1{}^\infty S + m_\infty + \tilde{Z}(S)\} \frac{dS}{S^2 - 1} \tag{A-8}$$

with $S = r \exp(i\theta)$, and $dS = ir \exp(i\theta)\, d\theta$. In the limit (A-8) reduces to

$$i\pi A_1{}^\infty. \tag{A-9}$$

Collecting (A-1), (A-2), (A-6), (A-7), and (A-9) and simplifying gives the result

$$Z(1) = \frac{2}{\pi}\int_0^\infty \frac{R(\Omega)}{\Omega^2 + 1}\, d\Omega + A_1{}^\infty + A_{-1}{}^0 + 2\sum_{k=1}^{L} \frac{A_{-1}{}^k}{1 + \Omega_k{}^2}. \tag{A-10}$$

Substitution of tan (θ) for Ω in (A-10) gives

$$Z(1) = \frac{2}{\pi}\int_0^{\pi/2} R(\theta)\, d\theta + A_1{}^\infty + A_{-1}{}^0 + 2\sum_{k=1}^{L} \frac{A_{-1}{}^k}{1 + \Omega_k{}^2}. \tag{A-11}$$

References

[1] P. I. Richards, "Resistor transmission line circuits," *Proc. IRE*, vol. 36, pp. 217–220, Feb. 1948.
[2] N. W. McLachlan, *Complex Variable Theory and Transform Calculus*. Cambridge, ch. 4, 2nd ed., 1963.
[3] H. Ozaki and J. Ishii, "Synthesis of a class of strip-line filters," *IRE Trans. on Circuit Theory*, vol. CT-5, pp. 104–109, June 1958.
[4] L. Young, "Tables for cascaded homogeneous quarter-wave transformers," *IRE Trans. on Microwave Theory and Techniques*, pp. 233–237, April 1959.
[5] H. Bode, *Network Analysis and Feedback Amplifier Design*. Van Nostrand, 1945.

A Note on the Finite-Element Solution of Exterior-Field Problems

Z. J. CSENDES, MEMBER, IEEE

Abstract—**An approximate closed-form expression corresponding to the energy functional in an infinite exterior region satisfying Laplace's equation is derived for use with the finite-element method. This expression simplifies the treatment of exterior-field problems in numerical calculations. The expression is given in terms of a few numerical matrices and logarithmic functions.**

I. Introduction

A number of problems in electromagnetics can be formulated in terms of an interior region and an exterior region satisfying Laplace's equation with boundary conditions at infinity. Several methods have been developed for the numerical treatment of these problems, including boundary relaxation [1]–[4], [7] and exterior finite-element methods [5], [6]. A common feature of all of these methods is the solution of the problem in terms of a finite, bounded region called a "picture frame" and the use of Green's functions to determine picture-frame boundary conditions.

Manuscript received September 18, 1975; revised November 24, 1975. This short paper is published with the permission of the General Electric Company.
The author is with the General Electric Company, Schenectady, NY 12345.

There are two competing approaches to the selection of picture-frame regions and the use of Green's function boundary conditions. In one approach, first proposed by Silvester and Hsieh [5], a single picture frame is defined and the energy-functional contribution of the entire region exterior to this picture frame is evaluated and added to the interior-region energy functional. The solution is therefore obtained by considering the field in all space, but by explicitly solving for the field only in the region interior to the picture frame. In the other approach, proposed by McDonald and Wexler [6], two concentric picture frames are defined and the integral equation relating the potentials between the two picture frames is used to specify the boundary conditions on the outer picture frame. Fields outside of the outer picture frame are never considered in the solution process; the integral equation merely provides a relationship between internal field values.

As developed in the references, however, the energy functional in the exterior region is evaluated by using an integral transformation and weighted Gaussian quadrature formulas. The programming requirements of this procedure are relatively difficult and have limited the application of the technique. In this short paper, the value of the exterior-field energy functional is expressed in closed form. The programming requirements of these closed-form expressions are much less than that of the original transformation-quadrature procedure; hence, the availability and utility of exterior-field finite-element solutions is increased.

II. The Exterior-Field Functional

It is shown in [5] that the energy functional corresponding to the exterior of a finite-element mesh embedded in a space where Laplace's equation applies is given by

$$\mathscr{F}_E = \boldsymbol{a}\boldsymbol{R}\boldsymbol{Q}^{-1}\boldsymbol{R}\boldsymbol{a}^T \tag{1}$$

where $\boldsymbol{a}$ is a row vector of potential coefficients on the edge of the finite-element mesh and $\boldsymbol{R}$ and $\boldsymbol{Q}$ are the symmetric matrices

$$\boldsymbol{R} = \oint \boldsymbol{\beta}^T(x)\boldsymbol{\beta}(x)\, dx \tag{2}$$

$$\boldsymbol{Q} = \oint\oint \boldsymbol{\beta}^T(x)G(x,\xi)\boldsymbol{\beta}(\xi)\, d\xi\, dx. \tag{3}$$

In these equations, $\boldsymbol{\beta}(x)$ is a row vector composed of the interpolation polynomials corresponding to the coefficients $\boldsymbol{a}$ and

$$G(x,\xi) = \frac{1}{2\pi\varepsilon} \ln |x - \xi| \tag{4}$$

where $|x - \xi|$ indicates the distance between point x and point ξ.

The matrices $\boldsymbol{R}$ and $\boldsymbol{Q}$ in (2) and (3) may be converted into finite-element form by noting that

$$\boldsymbol{\beta}(x) = \sum_{h=1}^{N} \boldsymbol{\beta}^{(h)}(x) \tag{5}$$

where $\boldsymbol{\beta}^{(h)}(x)$ is a row vector containing the interpolation polynomials for element h ($\boldsymbol{\beta}^{(h)}(x) = 0$ if x is outside element h) and N is the number of elements on the boundary. By making the substitution $z = x/L_h$ where L_h is the length of the exterior side of element h, the interpolation polynomials $\boldsymbol{\beta}^{(h)}(x)$ may be written as

$$\boldsymbol{\beta}^{(h)}(zL_h) = \boldsymbol{p}(z)\boldsymbol{\Gamma} \tag{6}$$